HAL
open science

Prediction of the compressive damage response of flax-reinforced laminates using a mesoscale framework

Constantin Nicolinco, Zia Mahboob, Yves Chemisky, Fodil Meraghni, Donatus Oguamanam, Habiba Bougherara

To cite this version:

Constantin Nicolinco, Zia Mahboob, Yves Chemisky, Fodil Meraghni, Donatus Oguamanam, et al.. Prediction of the compressive damage response of flax-reinforced laminates using a mesoscale framework. Composites Part A: Applied Science and Manufacturing, 2021, 140, pp.106153. 10.1016/j.compositesa.2020.106153 . hal-03784712

HAL Id: hal-03784712

https://hal.science/hal-03784712v1

Submitted on 23 Sep 2022

HAL is a multi-disciplinary open access archive for the deposit and dissemination of scientific research documents, whether they are published or not. The documents may come from teaching and research institutions in France or abroad, or from public or private research centers.

L'archive ouverte pluridisciplinaire **HAL**, est destinée au dépôt et à la diffusion de documents scientifiques de niveau recherche, publiés ou non, émanant des établissements d'enseignement et de recherche français ou étrangers, des laboratoires publics ou privés.

Prediction of the compressive damage response of flax-reinforced laminates using a mesoscale framework

Constantin Nicolinco [a], Zia Mahboob [b], Yves Chemisky [c], Fodil Meraghni [d], Donatus Oguamanam [b], Habiba Bougherara [b,*]

[a] Department of Aerospace Engineering, Ryerson University, Toronto, ON, Canada
[b] Department of Mechanical & Industrial Engineering, Ryerson University, Toronto, ON, Canada
[c] Université de Bordeaux, I2M UMR CNRS 5295, Bordeaux, France
[d] Arts et Meìtiers Institute of Technology, CNRS, Université de Lorraine, LEM3-UMR 7239, France

A B S T R A C T

Compressive mechanical testing was performed on continuous fiber Flax/Epoxy laminate specimens, capturing, and quantifying its evolving in-plane plasticity and moduli. This non-linear behaviour was simulated using a modified continuum damage mechanics-based model. The standard Mesoscale Damage Theory (MDT) of Ladeveze and Le Dantec was modified to include fiber-direction damage and plasticity evolution constitutive equations in order to capture the non-linear behavior observed in Natural Fiber Composites (NFCs). The model parameters were experimentally identified and optimized. Validations have been performed on Flax/Epoxy laminates of various fiber orientations, as well as on E-Glass/Polyester using data from available literature. The proposed model successfully predicts the NFCs nonlinear compressive mechanical response. It is a robust predictive tool to aid engineers and designers in the development of load-bearing biomaterial-reinforced composites.

1. Introduction and background

Continuous fiber-reinforced composites are a popular material of choice in industries partly because of their high specific strength and their near net-shape manufacturing property. E-Glass is the most widely used reinforcing fiber [1–7]. However, its need for energy-intensive manufacturing and their limited recyclability, amongst other drawbacks, have created an interest in the investigation of cost-effective and sustainable bio-based alternatives with a reduced environmental footprint [1,6,8–11]. Studies on the replacement of glass with natural fibers as composite reinforcement have been reported in the literature [1–4,6,8–17]. Several plant-derived fibers such as coconut, jute, hemp, sisal, and bamboo have shown promising mechanical properties, while being both economically and ecologically superior to glass [2,8,17].

For structural applications, flax has been identified to compare most favorably with E-Glass in the areas of specific strength (1300 vs 1350 MPa/gcm^{-3}), specific modulus (20–70 vs 30 GPa/gcm^{-3}), cost per unit weight (0.6 vs 1.2 USD/lb), cost per unit tensile strength (0.15 vs 0.17 USD /ksi), and cost per unit flexural strength (0.003 vs 0.003 USD/ksi) [2,4,18]. Environmentally, plant fibers are renewable, carbon dioxide neutral, easier to process, and easier to dispose of when compared to synthetic fibers [2–7]. Le Duigou et al. [5] directly compared the environmental impact resulting from the production of 1 kg hackled flax fiber versus glass fiber. Flax has been shown to be considerably less environmentally damaging in a variety of aspects such as abiotic depletion, acidification, eutrophication, global warming, ozone layer depletion, human toxicity, fresh water aquatic toxicity, photochemical oxidation, and terrestrial ecotoxicity. Furthermore, fiber production for composite-reinforcement purposes consumes 4 times less non-renewable energy when compared to E-Glass (11.7 MJ/kg vs 45 MJ/kg [5,17]).

Nonetheless, natural fiber reinforced composites (NFCs) are not used in structural and load-bearing applications due to incomplete and ongoing research in the areas of flammability and operating temperatures [4,19,20], biodegradability [3,6,9,15], hydrophilic properties [21–24], adhesion and surface treatments [22,24–28], and mechanical behavior [1,24,29–39]. Moreover, there is a noticeable scarcity of validated and reliable computational methods to model the non-linear behavior observed in NFCs [36]. The prediction of damage and plasticity progress (stiffness evolution), as well as the development of failure criteria, are crucial for the design process of engineering parts and components. Therefore, effective implementation of NFCs in load-

* Corresponding author.

bearing applications requires not only a profound understanding of their mechanical behavior, but also a robust predictive tool that is capable of accurately simulating the material response to subjected loads. The successful achievement of these goals will give engineers and designers the confidence in NFCs structural capabilities, and to promote the use of sustainable and eco-friendly materials.

1.1. Flax fiber

Originating in the Mediterranean regions of Europe, flax is one of the earliest domesticated crops. Even though its commercial production was successful in the 19th century, the invention of the cotton gin brought a decline to the flax industry [40–42]. Currently, flax is harvested for non-load-bearing applications such as consumption (seed and oil), clothing (linen), insulation, tableware, surgical threads, and paper [16,41].

Flax fiber is fundamentally composed of cellulosic polymers that are arranged into a complex hierarchical structure [19,33,43]. Elementary fibers are polygonal in shape, with a hollow central part (lumen). Technical fibers are composed of 10 to 40 elementary fibers held by a pectin (glue-like) layer [19]. The complex hierarchical and layered structure of flax, as well as the heterogenic nature of elementary fibers, yield a complex damage progression and nonlinear plastic behavior [16,31,36,44]. The bulk of the fiber (circa 70%) consists of microfibrils spiraling around the central lumen at a 10-degree orientation [19,43]. Under tensile loads, Bayle as well as others [29,36,37] observed fiber stiffening as well as plasticity; where the fiber modulus varies as the microfibrils irreversibly re-orient themselves towards the load-axis. Moreover, under cyclic loading, the fiber modulus was reported to experience a 60% to 80% increase between the first and last cycle [45]. Compressive tests on single perfect and imperfect fibers showed that circumferential kink bands are irreversibly produced as a response to such loads [29]. The bands severely degrade the fiber compressive mechanical properties, and often present the fiber's principal failure region [31,34,36,45,46]. As observed by Bos and Donald [33], kink band formation is characteristically a plastic deformation. Even if the fiber starts defect free, kink band formation within the primary cell wall eventually leads the fiber to failure in buckling [36]. Flax fibers are known to have a wide range of mechanical properties, as seen in the literature surveys compiled by Mahboob et al. in accordance with others [4,8,9,15,16,36,46,47]. This is due to variations in specimen length, moisture levels, imperfections, origin, and heterogeneous fiber geometry [29,36,38,47–49]. Noting that even though the fibers reported compressive strengths are within a desirable range, the scarcity of data (less than a handful) severely degrades the confidence in its applications. This further solidifies the need of compressive research conducted on flax.

1.2. Flax composites and damage mechanisms

Some flax-composites can be found in large-scale industries. A common automotive application is to blend short flax fibers in a thermoplastic matrix, and compression mold the non-woven mats into door panels, window pillars, package trays, and trunk liners [9,12,16]. Other flax-composites consumer products manufactured in lesser quantities include musical instruments, and sporting goods such as snowboards, canoes, hockey sticks and more [16]. There is a growing interest to produce load-bearing flax components, which is seen in many prototype projects such as the 100% biodegradable vertical windmill [50] and the University of Stuttgart flax wind-turbine blades [51]. However, as previously mentioned, the use of flax fibers in load-bearing applications is limited by two major factors: a knowledge gap in its mechanical behavior, and a lack of practical modeling tools.

Due to its hydrophilic nature, flax has a poor interfacial adhesion strength with generic synthetic polymer thermosets [4,20,26,45]. Surface treatments could be implemented to strengthen the fiber-matrix bond; however, this often comes at a price of reduced composite strength due to inflicted damage on treated fibers [4,9,22,28]. On the other hand, high performance epoxies have been shown to have a good adhesion strength to natural fibers and are an excellent matrix candidate for load-bearing NFCs [25]. Unlike conventional materials such as metals and polymers, composites fail from a variety of independent or coupled mechanisms. Local failures are referred to as damage, physically represented as local discontinuities manifesting as voids and cracks [52,53]. Fibrous composites have been observed to firstly develop damage on the micro scale through fiber fracture, splitting, pull-out, and interfacial deboning [44,52]. Microscale failures eventually evolve into macroscale failures such as transverse cracks, matrix rapture, and delamination. In compression, macroscale NFC failure is a function of both fiber and matrix properties. Here, the matrix prevents fiber buckling while the fiber-matrix adhesion prevents matrix rapture [54]. The nonlinear behavior observed in flax fibers is known to transfer to flax composites, resulting in a nonlinear stiffness variation (Young's modulus deterioration and recovery) [39,44]. On the microscale, Bos et al. [45] in accordance with Mahboob et al. [36] identified inter-microfibril adhesion as the primary failure mode in flax and flax/epoxy composites. Elementary fibers as well as microfibrils within the S2 layer come apart much like a compressed steel cable, while the matrix remained virtually crack-free. On the macro level, Mahboob et al. [36] identified debonding and delamination as the primary failure mechanisms preceding buckling. Fiber bundles and matrix-rich regions remained crack free, while cracks developed along the fiber-matrix interface [36].

1.3. NFC modelling

NFCs have been successfully modeled using semi-empirical models and polynomial-type failure criteria. Facca et al. [55] compared several NFCs' experimental Young's moduli and tensile strengths with theoretical predictions from various micromechanical models (rule-of-mixtures, Halpin-Tsai, Nairn's generalized shear-lag analysis and Mendels stress transfer models) and obtained mixed results that improved with the implementation of several correction factors. Anderson et al. [56] simulated the macroscopic behavior of flax laminates by fitting a stress-strain relationship to experimental observations of a singly ply, and then using classical laminate theory to simulate the overall laminate response. This macroscopic approach yielded reasonable accuracy with the exception of cross-ply ($\pm 45^{\circ}$) laminates, where ply re-orientation was identified as an unaccounted damage mechanism. Panamoottil et al. [57] proposed a semi-empirical CDM (Continuum Damage Mechanics) model to predict the tensile response of UD (Uni-Directional) flax laminates. Progressive stiffness variation was incorporated using a material damage tensor, which represents fiber crack densities that were directly measured from tested specimens. The model was found to poorly reproduce a single-ply behavior, with improved results for a 5-ply laminate. Recently, Poilane et al. [58] developed a visco-elasto-plastic model that incorporated CDM and thermodynamics considerations. It was assumed that the nonlinear response of a flax/epoxy laminate is captured by visco-plastic effects which were described by combined linear-nonlinear hardening functions. A similar approach was used by Sliseris et al. [59] who proposed a CDM-based thermodynamic micromechanical model to simulate the mechanical behavior of a single-ply woven flax/epoxy composite. Both matrix and reinforcement were

modeled using nonlinear plasticity constitutive equations with isotropic hardening laws. Again, no state variables were used to quantify material property degradation, and visco-plastic effects where used to describe the material's nonlinear behavior. The model proved captured the main damage mechanisms of set composite and good agreement was observed between the simulations and experimental results. It is worth noting that while the previously mentioned CDM-based models captured the material response with good accuracy, they assumed the composite's modulus to be constant. This assumption is questionable as flax fibers have been observed to suffer damage and to experience material property deterioration as previously discussed. In a recent paper, Mahboob et al. [44] developed a CDM-based model within a thermodynamics framework that captured the tensile response of flax/epoxy laminates for various fiber orientations. Based on the mesoscale damage theory described by Herakovich [53], the modified theory includes separately-formulated damage and plasticity evolution constitutive equations, which proved to be accurate as well as versatile.

All the aforementioned models exclusively targeted the tensile behavior of NFCs. Investigations on the compressive behavior of natural fiber reinforced composites are rare. Nonetheless, it is evident that the complex behavior exhibited by flax-reinforced composites can be modeled using thermodynamic CDM-based techniques. In this study, a thermodynamic CDM-based modified mesoscale damage model is developed and used to simulate the nonlinear compressive response of flax/epoxy laminates of various fiber orientations. This is achieved through the independent formulation of fiber direction and coupled shear-transverse direction damage and plasticity constitutive equations. Stiffening and plasticity evolution laws are defined from experimental observations, while model parameters are derived from experimental data and optimized using an open-source algorithm.

2. Experimental procedure

Due to the bio-nature of the material, conventional techniques for volume fraction calculations such as matrix incineration or digestion in acid are inapplicable. An SEM (Scanning Electron Microscopy) was used to determine the fiber, matrix, and void volume fractions under the assumption that area fractions are accurate representations of volume fractions.

2.1. Manufacturing

Unidirectional FlaxPly® fabric with a weight to area ratio of 150 g/cm^2 was used to fabricate 16-layer composite specimens with a 50% fiber volume fraction. As shown in Fig. 1, the fabric consisted of a 40 to 3 warp to weft strand ratio. Each strand is a bundle of elementary fibers twisted to an average of 5 turns/cm. Quasi-static testing revealed that while the presence of the weft strand had a negligible influence on the basic mechanical properties of the composites, it ensured that the warp yarn's alignment remained true. A high performance, hot curing thermoset epoxy supplied by Huntsman Corp. (The Woodlands, TX, USA) was used as the matrix material. It comprises Araldite® LY5 epoxy resin and Aradur® 22962 hardener and presents unprecedented mechanical performance and bond strength.

Specimens with $[0]_{16}$, $[90]_{16}$, $[\pm 45]_{4s}$, and $[\pm 67.5]_{4s}$ orientations and 4 mm in thickness were manufactured through compression molding and cut according to ASTM D6641/D6641M guidelines [60]. Fig. 2 is a schematic of the composite plate's consolidation setup and the test specimen. Epoxy only specimens were manufactured into dog-bone shapes following ASTM D695-15 [61] geometry standards. The expected strains were beyond the available strain gauge and extensometer capabilities; therefore, Digital Image Correlation (DIC) techniques were used to quantify the material strain. The specimens where covered with a fine random speckle pattern and a high-resolution camera tracked the motion of set speckles over the course of the load history. The camera was placed sufficiently far away from the samples to minimize out-of-plane bulging effects. The images were recorded every 50 ms, and an off-the-shelf DIC software was used to analyze the images and obtain the digital extensometer readings.

2.2. Quasi-static testing

To capture the specimen's evolving modulus and plasticity, repeated cycles of load/unload were performed with progressively increasing loads up to complete failure. All tests were performed at room temperature and pressure using a servo-hydraulic test frame (MTS 322, Eden Prairie, MN, USA) at a displacement rate of 2 mm/min. Fig. 3 illustrates the testing setup - note that the material's hysteretic response curves (thin blue lines) is approximated as linearly elastic (red dash lines). The specimen's elastic modulus (E) degrades with each cycle, which permits the characterization of the material's damage and plasticity evolution.

3. New damage model

Given that both micro and macro scale failures are present in NFCs, accurate modeling requires a physics-based theory that is capable of capturing damage and plasticity on a scale that is between the two extremes. These models are known as the *mesoscale*.

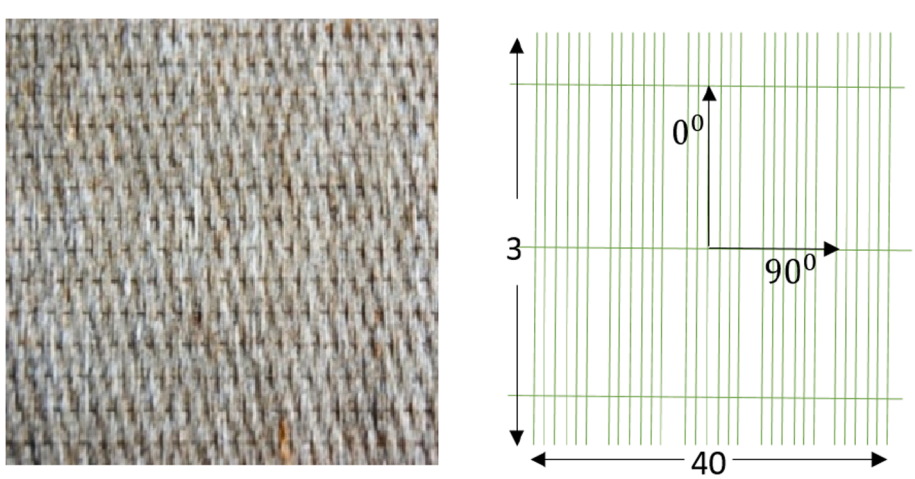

Fig. 1. Dry UD FlaxPly® fabric photo (left) and schematic (right). (For interpretation of the references to colour in this figure legend, the reader is referred to the web version of this article.)

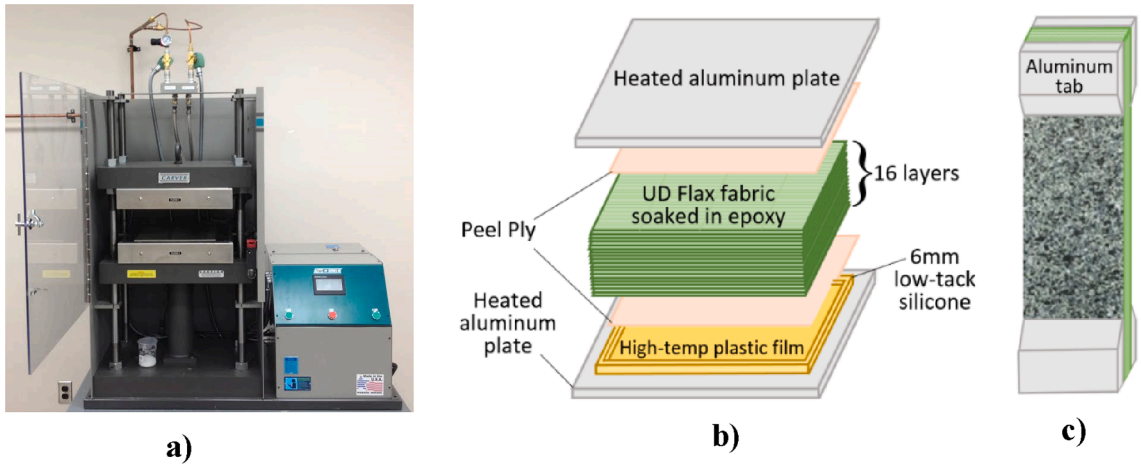

Fig. 2. Composite manufacturing setup: a) Compression molding machine, b) lay-up, c) test specimen with Aluminum tabs and speckled pattern sprayed of the outer surface for DIC measurements. (For interpretation of the references to colour in this figure legend, the reader is referred to the web version of this article.)

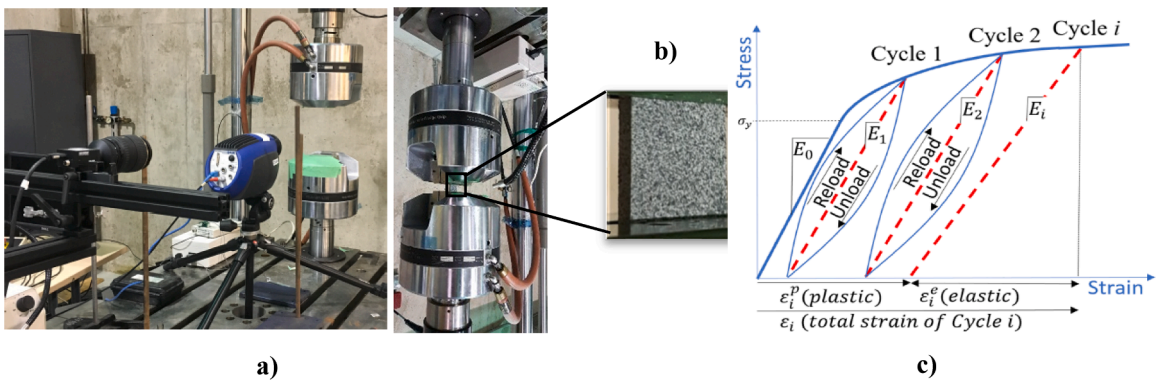

Fig. 3. Schematic representation of the test setup: a) test frame, b) tested specimen mounted on the grips, and typical response of NFC under load-unload conditions showing an evolving elastic modulus. (For interpretation of the references to colour in this figure legend, the reader is referred to the web version of this article.)

3.1. Standard mesoscale damage theory

The standard Mesoscale Damage Theory (MDT) proposed by Ladeveze & Le Dantec [62] is one the most popular, robust, and versatile continuum damage mechanics (CDM) based theories. The Model is founded on the principle of irreversible thermodynamics, where local material states are expressed in terms of state variables and associated thermodynamic forces. The MDT assumes that the material's mechanical response is fully expressed in terms of its degrading elastic moduli (damage) and the accumulated permanent strains (plasticity). Any damage and plasticity evolution are a succession of the previous equilibrium state and does not depend on time derivatives of state variables.

The theory considers two distinct elementary components: layers of composites and the interface between them. Damage states are allowed to vary in between layers, but they remain consistent throughout a given layer. Damage evolution laws are material-dependent, and they reflect basic material properties and dominant damage mechanisms. The theory is phenomenological since it does not consider the individual damage mechanisms, but rather uses experimental observations to characterize the cumulative damage evolution. It has been successfully applied to polymeric, ceramic, and metallic composites reinforced with short fibers, long fiber, and fabrics. A detailed MDT description can be found in the book by Herakovich [53], along with validated examples. Note that the standard MDT model defines damage variables only for transverse and shear planes. Since it was originally formulated for synthetic fiber composites where the reinforcing fibers tend to be linear-elastic and brittle materials, fiber- direction modulus degradation is not typically defined. Also, no plasticity is allowed for in the fiber-direction and only the transverse and shear permanent deformation is defined in MDT model. Experimental tests conducted by Mahboob et al. [36] confirmed that flax – composites exhibit progressive modulus degradation and inelastic deformation along fiber-direction, in-plane transverse and shear deformation under tensile and compression loading. Therefore, it is necessary to modify the standard model.

3.2. Modified mesoscale damage theory

The Mesoscale Damage Theory (MDT) considers each ply as an orthotropic elastic-plastic material, where damage is uniformly distributed and evolving throughout the ply. Damage is represented as stiffness deterioration, and, as previously stated, damage states are consistent within each ply, but are allowed to vary between plies [53].

3.2.1. Single-Ply

In the case of quasi-static mechanical deformation of orthotropic materials under isothermal condition, the thermodynamic potential function, which is derived from *Gibbs Free Energy*, may be expressed as the elastic strain energy E_D. This function is used to build lamina damage model for anisotropic material like fiber-composite. Mahboob et al. [44] adopted the formulation of elastic strain energy presented by Herakovich [53] to describe the in-plane tensile response in fiber direction. These formulations assume that the compression modulus remain constant, which does not reflect actual NFC response based on experimental observations [36]. Here, the 3D formulation is further modified to

incorporate ply in-plane damage evolution only by assuming that damage affects the elastic strain energy of material in both tension and compression:

$$2E_D = \frac{\sigma_{11}^2}{E_{11}^0(1-D_{11})} - 2\frac{\nu_{12}}{E_{11}}\sigma_{11}\sigma_{22} - 2\frac{\nu_{13}}{E_{11}}\sigma_{11}\sigma_{33} + \frac{\sigma_{22}}{E_{22}^0(1-D_{22})} - 2\frac{\nu_{32}}{E_{33}}\sigma_{22}\sigma_{33} + \frac{\sigma_{33}{}^2}{E_{33}} + \frac{\sigma_{12}^2}{G_{12}^0(1-D_{12})} + \frac{\sigma_{13}^2}{G_{13}} + \frac{\sigma_{23}^2}{G_{23}} \tag{1}$$

where the following functional relationships apply: $\frac{\nu_{12}}{E_{11}} = \frac{\nu_{21}}{E_{22}}, \frac{\nu_{13}}{E_{11}} = \frac{\nu_{31}}{E_{33}}$, *and* $\frac{\nu_{32}}{E_{33}} = \frac{\nu_{23}}{E_{22}}$. The subscript 1, 2 and 3 denote respectively the fiber direction, the transverse direction and normal direction. D_{11}, D_{22} and D_{12} are in-plane damage components along the fiber direction, perpendicular to fiber direction (transverse) and shear plane, respectively. E_{11}, E_{22} and G_{12} are damaged elastic moduli which are expressed in terms of corresponded damage variable D_{11}, D_{22}, D_{12} and initial elastic modulus E_{11}^0, E_{22}^0 and G_{12}^0. Thus, the effective stress σ for an in-plane loading condition is written as follows:

$$\sigma_{11} = \frac{\sigma_{11}}{1-D_{11}}$$

$$\sigma_{22} = \frac{\sigma_{22}}{1-D_{22}}$$

$$\sigma_{12} = \frac{\sigma_{12}}{1-D_{12}} \tag{2}$$

Using the principle of strain equivalence as presented in [63], the elastic constitutive equations for the effective elastic strain ε^e are given by:

$$\varepsilon_{11}^e = \frac{\partial E_D}{\partial \sigma_{11}} = \frac{\sigma_{11}}{E_{11}^0(1-D_{11})} - \frac{\nu_{12}}{E_{11}}\sigma_{22}$$

$$\varepsilon_{22}^e = \frac{\partial E_D}{\partial \sigma_{22}} = \frac{\sigma_{22}}{E_{22}^0(1-D_{22})} - \frac{\nu_{12}}{E_{11}}\sigma_{11} \tag{3}$$

$$\varepsilon_{12}^e = \frac{\partial E_D}{\partial \sigma_{12}} = \frac{\sigma_{12}}{2G_{12}^0(1-D_{12})}$$

The associated thermodynamic forces (i.e., the damage energy release rates) of the three in-plane damage variables in a single ply are defined such that a given damage threshold must be exceeded in order for additional damage to occur:

$$Y_{11} = \frac{\partial E_D}{\partial D_{11}} = \frac{\sigma_{11}^2}{2E_{11}^0(1-D_{11})^2}$$

$$Y_{22} = \frac{\partial E_D}{\partial D_{22}} = \frac{\sigma_{22}^2}{2E_{22}^0(1-D_{22})^2} \tag{4}$$

$$Y_{12} = \frac{\partial E_D}{\partial D_{12}} = \frac{\sigma_{12}^2}{2G_{12}^0(1-D_{12})^2}$$

As noted earlier, typical MDT formulations presented in [53,62] assume no damage development in the fiber direction, which is questionable for flax. Therefore, constitutive equations for damage development in the fiber direction are introduced, fully decoupled from shear-transverse direction similar to that defined by Mahboob et al. [44]:

$$Y_f = \sqrt{Y_{11}} \quad \& \quad Y_{ts} = \sqrt{Y_{12} + b_{ts}Y_{22}} \tag{5}$$

where b_{ts} is a shear-transverse coupling parameter, and *f, t,* and *s* denote the fiber, transverse, and shear directions, respectively.

In the standard MDT model, the evolution of the coupled damage force is defined as a function of each damage variable D_{22}, D_{12} separately and assumed to be linear. Similarly, in this study, experimental observations revealed that the flax/epoxy compressive damage evolution law (Φ_{D_i}) follows a linear trend; hence they are formulated as follows:

$$\Phi_{D_{11}} = \frac{Y_f - Y_f^0}{Y_f^c} - D_{11} \leq 0, \quad \text{if } \sigma_{11} \leq 0, \quad \varepsilon_{11} < \varepsilon_{11}^{max}; \quad \text{otherwise } D_{11} = 1$$

$$\Phi_{D_{22}} = \frac{Y_{ts} - Y_t^0}{Y_t^c} - D_{22} \leq 0, \quad \text{if } D_{22} < 1, \quad Y_{22} < Y_{22}^{max},\ Y_{12} < Y_{12}^{max}; \quad \text{otherwise } D_{22} = 1 \tag{6}$$

$$\Phi_{D_{12}} = \frac{Y_{ts} - Y_s^0}{Y_s^c} - D_{12} \leq 0, \quad \text{if } D_{12} < 1; \quad Y_{22} < Y_{22}^{max},\ Y_{12} < Y_{12}^{max}; \quad \text{otherwise } D_{12} = 1$$

where ε_{11}^{max} is the compressive ultimate strain in the fiber-direction. Superscripts *C* and *0* represent the critical and initial values, while $Y_f^0, Y_f^C, Y_t^0, Y_t^C, Y_s^0, Y_s^C, Y_{22}^{max}$ and Y_{12}^{max} are material parameters to be identified. The damage evolution occurs during the damage variable range from 0 to 1, where $D_{ij} = 1$ indicates the complete damaged material.

Unlike synthetic fibers, flax has been observed to develop plasticity (permanent strains) throughout its load history. Standard MDT formulation is adopted as illustrated in Fig. 3, where the total strain is decomposed into elastic ε^e and plastic ε^p strains for each of the three orthotropic direction. The effective inelastic strain rates are defined in terms of damage as follows:

$$\dot{\varepsilon}_{ij}^{P} = \dot{\varepsilon}_{ij}^{P}(1-D_{ij}), \quad \text{for} \quad i, j \in (1,2) \tag{7}$$

In order to define the elastic domain (i.e., yield surface), two functions Φ_f^p and Φ_{ts}^p are introduced to indicate the plasticity evolution in the fiber-direction and shear-transverse, respectively. Similar to damage formulations, the fiber-direction placticity evolution Φ_f^p is fully decoupled from shear-transverse direction. The coupled shear-transverse plasticity evolution Φ_{ts}^p remained as in the standard MDT formulations [53]:

$$\Phi_f^p = \tilde{\sigma}_f^{eq} - h_f(\tilde{p}_f) - \sigma_f^0 \leq 0, \quad \dot{\tilde{p}}_f \geq 0$$

$$\Phi_{ts}^p = \tilde{\sigma}_{ts}^{eq} - h_{ts}(\tilde{p}_{ts}) - \sigma_{ts}^0 \leq 0, \ \dot{\tilde{p}}_{ts} \geq 0 \tag{8}$$

where σ_f^0 and σ_{ts}^0 are the initial size of the yield surface to be determined experimentally for the onset of plasticity. While σ_f^{eq} and σ_{ts}^{eq} are equivalent stresses in the fiber and shear-transverse directions, formulated as in standard MTD publications [53,62]:

$$\tilde{\sigma}_f^{eq} = \frac{\sigma_{11}}{1-D_{11}} \quad \& \quad \tilde{\sigma}_{ts}^{eq} = \sqrt{\frac{\sigma_{12}^2}{(1-D_{12})^2} + \frac{A_{ts}\sigma_{22}^2}{(1-D_{22})^2}} \tag{9}$$

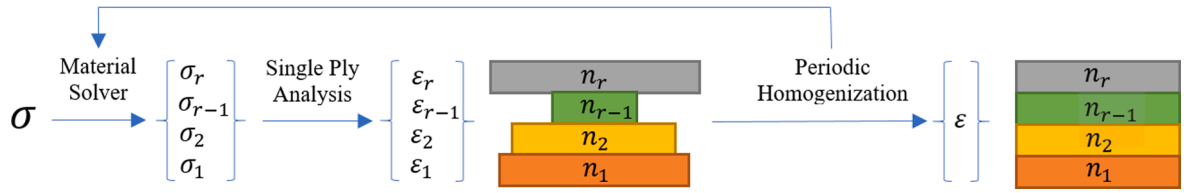

Fig.4. Multi-ply modeling schematic. (For interpretation of the references to colour in this figure legend, the reader is referred to the web version of this article.)

where A_{ts} is a linear shear-transverse coupling parameter, $h_f\left(\tilde{p}_f\right)$ and $h_{ts}(\tilde{p}_{ts})$ are hardening functions dependent on the accumulated effective inelastic strains in the fiber direction ($\left(\tilde{p}_f\right)$) and shear-transverse direction ($\tilde{p}_{ts}$). Both have been observed to follow a power law trend, and they are formulated as follows [53,62]:

$$h_f(\tilde{p}_f) = \beta_f(\tilde{p}_f)^{\alpha_f} \quad \& \quad h_{ts}(\tilde{p}_{ts}) = \beta_{ts}(\tilde{p}_{ts})^{\alpha_{ts}} \tag{10}$$

where β_f, β_{ts}, α_f and α_{ts} are unknown parameters.

3.2.2. *Multi-Ply model and implementation*

As in previous work of Mahboob et al. [44] regarding flax modeling in tension, the multi-ply response is determined using periodic homogenization theory. This approach can account for 3D loading conditions and has is effective for materials with highly non-linear response such as shape-memory alloy composites. The model was implemented using open-source C++ SMART+ libraries (Smart Materials Algorithms and Research Tools [64]) developed by several collaborating institutions. It makes use of the convex cutting plane algorithms proposed by Simo and Hughes [65], and solves a set of five nonlinear equations (3 for damage (Φ_D) and 2 for plasticity (Φ^P) using numerical schemes as presented in

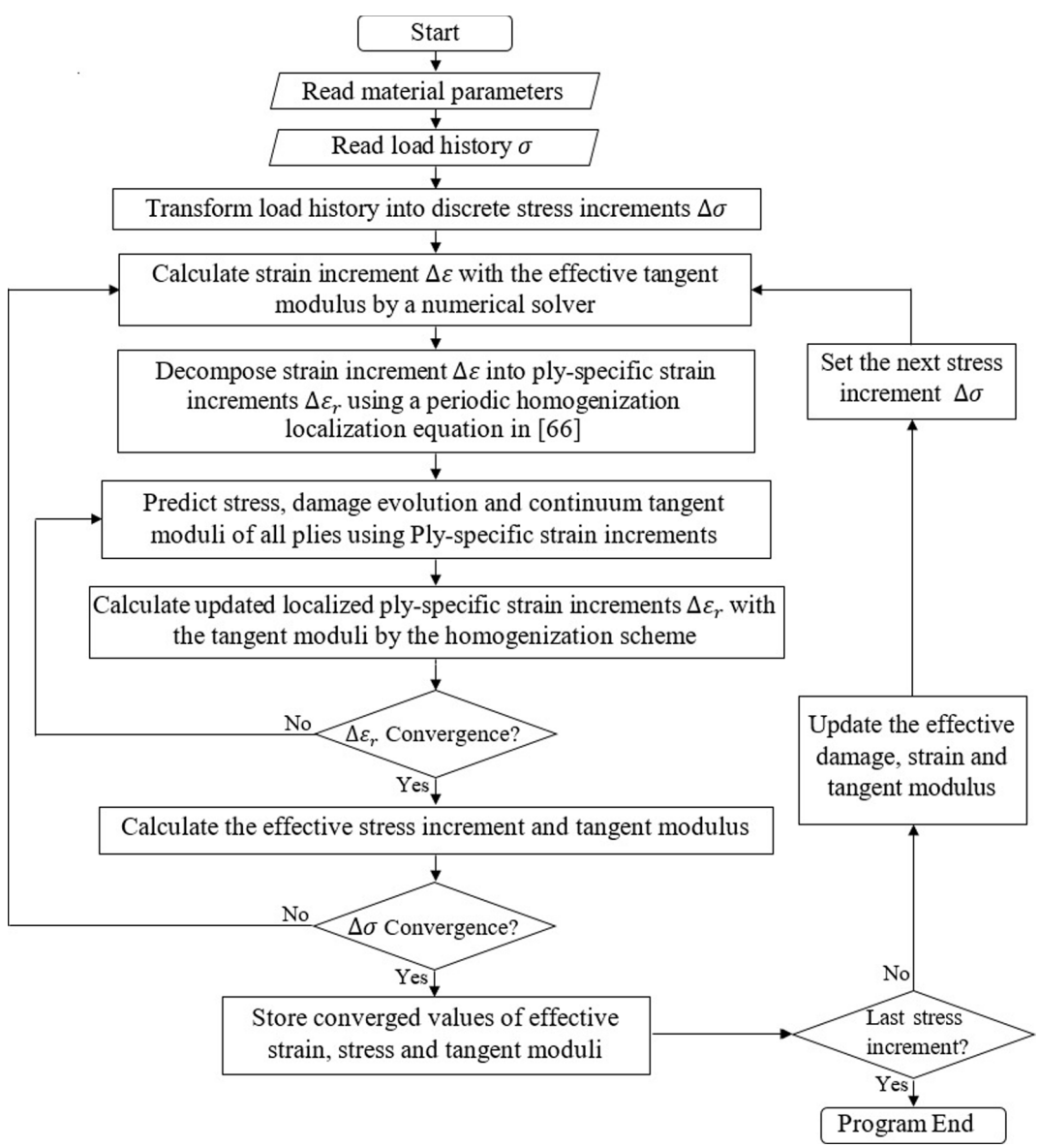

Fig. 5. Flowchart of the mesoscale damage model algorithm.

[66]. The working principle behind multi-ply modeling is illustrated in Fig. 4. The exact stress state of each ply is required in order to calculate the strain rate. This is unknown since the input parameter of the software is the total composite stress. The total composite stress is therefore decomposed into ply-specific stresses via the use of a material solver. Thereafter, ply-specific analysis is performed as described in Section 3.2.1; however, there is a chance of strain mismatch due to an inaccurate initial stress decomposition. Hence, the SMART+ periodic homogenization algorithms are applied to the resulting strains to iteratively modify the ply-specific stress increments until the resulting ply strains are equivalent.

The overall modeling process can be interpreted as a dual-stage iterative procedure. The first stage deals with individual plies, iterating the damage and plasticity states of each ply. The second stage is at the laminate level, where iterations are performed on ply-specific stress components in order to achieve a uniform strain state within the composite. A schematic representation of the whole iteration process including all the calculation steps is shown in Fig. 5.

3.3. Flax-reinforced composites characteristics

In order to determine the material properties and parameters, standard MDT publications recommend performing cycled load-unload tests on four types of laminates: $[0]_{16}$, $[90]_{16}$, $[\pm 45]_{4s}$, and $[\pm 67.5]_{4s}$ [53]. A comprehensive study of the flax/epoxy tensile and compressive material characteristics of these fiber orientations can be found in the work of Mahboob et al. [36]. The tested specimens, as shown in Fig. 6, did not buckle under quasi-static compression, but displayed different modes of failure.

3.3.1. Damage and plasticity in compression

The following observations were used in the formulations of the damage and plasticity evolution constitutive model equations. A total of 7 tests (monotonic and cyclic) were performed on 0^0 fiber-oriented specimens. Applying the MDT in reverse as described in [53] revealed the material's damage and plasticity evolution trends as seen in Fig. 7a and 7b, respectively. It is clearly noticeable that the compressive flax/epoxy damage evolution is linear, in contrast to the experimental tensile behavior reported by Mahboob et al. [44]. In accordance with [36], this further demonstrates that flax damage mechanisms are different in tension and compression. Plasticity was observed to evolve according to a power law with a positive fractional exponent, similarly to the tensile case reported in [44]. Cross-ply specimens were found to follow linear damage evolutions and power-shaped plasticity evolutions, whereas transverse fiber-oriented samples exhibited exponential damage and plasticity trends. This raised a substantial problem, as the MDT is fundamentally formulated with linear shear-transverse coupling parameters (b_{ts}, A_{ts}) as seen in Eqs. (5) and (9). Therefore, the theory intrinsically requires shear and transverse damage and plasticity evolutions to follow similar types of equations. Fortunately, a linear fit for damage evolution and a power-shaped plasticity evolution with a very small curvature were found to fit sufficiently well.

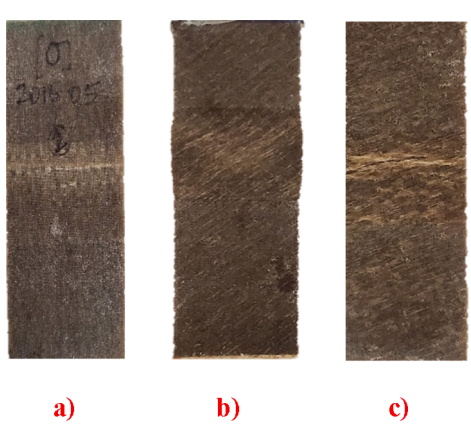

Fig. 6. Photographs of the tested specimens showing their failure modes: a) $[0]_{16}$, b) $[\pm 45]_{4s}$, and c)$[\pm 67.5]_{4s}$. (For interpretation of the references to colour in this figure legend, the reader is referred to the web version of this article.)

3.3.2. Parameter identification

Several parameters such as the undamaged elastic moduli, Poisson's ratios, and ultimate strains were extracted directly from the experimental data. Next, the experimental data was used to derive a good initial guess for the remaining parameters, as shown in the works of Herakovich [53]. An open-source global optimizer developed by Storn & Price [67] was imported from open source SciPy optimize differential evolution libraries [68]. It was used to refine the parameters to a satisfactory margin of error by slightly varying the parameters and quantifying the difference between experimental and simulated results. Since the experimental data and the model output have the same number of discrete points, the following equation was used as a simple cost function (*C.F.*), minimizing the difference between the experimental and predicted strain for each increment of stress:

$$C.F. = \sum_{i=1}^{i=m}\left[a\left(\sum_{i=1}^{i=n}\left|\varepsilon_L^{exp} - \varepsilon_L^{model}\right|\right) + (1-a)\left(\sum_{i=1}^{i=n}\left|\varepsilon_T^{exp} - \varepsilon_T^{model}\right|\right)\right] \quad (11)$$

where m is the number of specimens of different orientations, n is the number of discrete stress increments per specimen, L is the longitudinal direction, T is the transverse direction, and a is a weight factor biased to give priority to a better fit in the longitudinal direction. The optimized compressive flax/epoxy material-specific model parameters are presented in Table 1.

4. Results, validation, and discussion

4.1. Model validation on E-glass laminates

In this study, flax composites are introduced as an alternative to glass-reinforced composites. Therefore, compression validation was performed on E-Glass/Polyester laminates with various fiber orientations (Fig. 8a). To further demonstrate the versatility and robustness of the model, it was also applied to E-Glass/Epoxy laminates in tension (Fig. 8b). Experimental data was obtained from the works of Amijima & Adachi [69], while the damage and plasticity evolutions were given linear and power law formulations as in the standard MDT publications for brittle fibers [53,62]. It is observed that the present model successfully and accurately simulates the material response of glass-reinforced composites of various fiber orientation, subjected to both tensile and compressive loads. The damage, plasticity, and coupling parameters were identified using the optimization method discussed earlier. Thus, the model incorporates the material's nonlinear response rather than using linear-elastic approximation as in Ladeveze & Le Dantec [62]. From Fig. 8, it is observed that the model (solid black line) successfully predicts the E-Glass composite mechanical response to tensile and compressive loads, even at strains as high as 3%.

4.2. Flax laminates modelling

It can be inferred from Fig. 9 that there is an excellent agreement between the experimental and simulated results for the majority of the flax laminates; which includes predictions of stiffness loss (damage) and permanent deformations (plasticity) for longitudinal (right side) and transverse (left side) directions even at strain rates as high as 3%. In the case of the 90^0 fiber-oriented laminates, the model predicts the overall strain state of the material but cannot accurately decompose it into its elastic and plastic components. This is an outcome of the fundamental

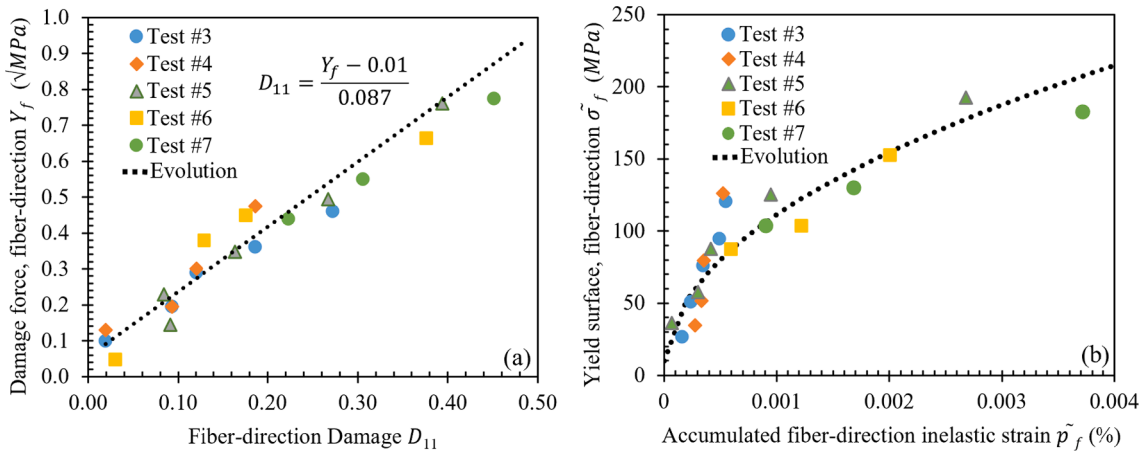

Fig. 7. Compressive fiber-direction evolution laws for unidirectional flax/epoxy specimens, (a) damage and (b) plasticity. (For interpretation of the references to colour in this figure legend, the reader is referred to the web version of this article.)

Table 1
Compressive flax/epoxy material-specific parameters.

Material properties	Value
ε_{11}^{max}	1.6%
E_{11}^0	32 GPa
E_{22}^0	5.23 GPa
G_{12}^0	1.66 GPa
ν_{12}^0	0.087
ν_{21}^0	0.396
Fiber-direction damage	
Y_f^0	$0.01\sqrt{\text{MPa}}$
Y_f^C	$1.64\sqrt{\text{MPa}}$
Fiber direction yield and plasticity	
σ_f^0	5.653 MPa
α_f	0.445
β_f	2998
Shear damage	
Y_{12}^{max}	1.26 MPa
Y_s^0	$0.001\sqrt{\text{MPa}}$
Y_s^c	$2.32\sqrt{\text{MPa}}$
Transverse coupled damage	
b	0.8
Y_{22}^{max}	5.03 MPa
Y_t^0	$0.0128\sqrt{\text{MPa}}$
Y_t^C	$2.65\sqrt{\text{MPa}}$
Transverse-shear plasticity	
A_{ts}	0.79
σ_{ts}^0	10.503
α_{ts}	0.45
β_{ts}	1170

difference in the transverse-fiber specimen plasticity evolution. As previously discussed in Section 3.3.1, the transverse fiber-oriented specimens exhibited a plastic evolution that is best fitted by an exponential function, while all others experienced a power-law relation with a fractional exponent. The current shear-transverse coupling constant A_{ts} is linear in nature, and, therefore, it cannot transform the power-shaped plasticity evolution curve into an exponential function for this fiber orientation. This is however not a major concern since there are limited scenarios where fiber reinforcement is aligned perpendicular to the load-axis. Moreover, the model can predict the overall strain state of the transverse fiber-oriented composite if this case is encountered.

Of note is the discrepancy noticed in the transverse-direction (left side) part of the $\pm 45^0$ fiber-oriented model. This phenomenon was observed in other works dealing with such cross-ply laminates, and it is attributed to the rotation of plies towards the load axis [44,56]; a mechanism unaccounted for in the present model. This discrepancy is substantially more severe than the one shown for a tensile case [44]. Therefore, it is postulated that other unaccounted damage mechanisms such as buckling severely influence this layup. Lastly, only one experimental cycle is shown for each type of laminate in order to maintain clarity for demonstrative purposes. Due to the nature of NFCs and their manufacturing procedures, there is some scatter in the material properties compared to typical metals, even if the specimens are cut from the same composite plate [37]. Therefore, some deviations between a specific specimen behavior and the average material behavior should be expected. Nonetheless, the observed good agreement between the experiments and simulations demonstrates that the damage and plasticity evolution laws developed for this model, accurately capture the nonlinear compressive response exhibited by NFCs.

4.3. Discussion

The mesoscale model presented in this study acts on the level of individual plies. Situated in between the micro and macro scales, the model quantifies the damage and plasticity states of each ply using dedicated state variable for all three orthotropic directions. This removes the oversimplifications of the macroscale models and avoids the computational difficulties often associated with micromechanics-based models. The standard MDT is modified to include the damage and plasticity evolution equations in all three orthotropic directions. The experimental results provided insight on the role of each damage and plasticity parameter on the individual damage and plasticity behavior for each ply, and for each of the three principal orthotropic directions. This can further be used to study the contribution of each ply to the overall laminate behavior and to develop highly optimized laminates with heterogeneous plies.

The overall laminate response was obtained by integrating each individual ply's response using a multi-scale periodic homogenization scheme. Flax-epoxy specific material parameters were identified by applying an optimization algorithm with a simple minimization cost function to the homogenization scheme. The resulting model and set of parameters successfully simulated the compressive response of flax/epoxy laminates of various fiber orientations. Moreover, the robustness and versatility of the model was shown through the ease of adaptation and accurate simulation of E-glass reinforced composites subjected to tensile and compressive loads.

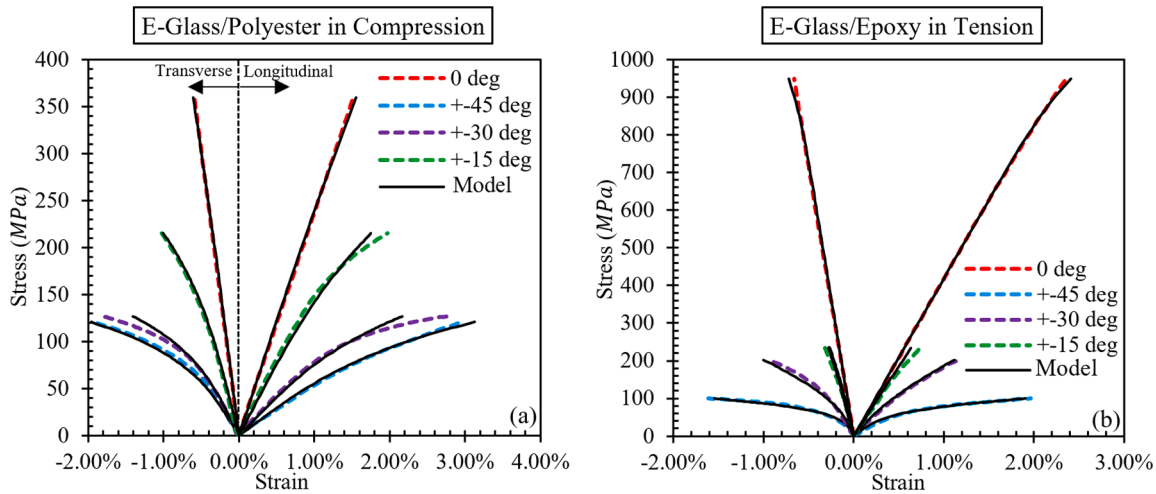

Fig. 8. Comparison of E-Glass laminate experimental material response (colored) and model simulation (black) in (a) compression, (b) tension. (For interpretation of the references to colour in this figure legend, the reader is referred to the web version of this article.)

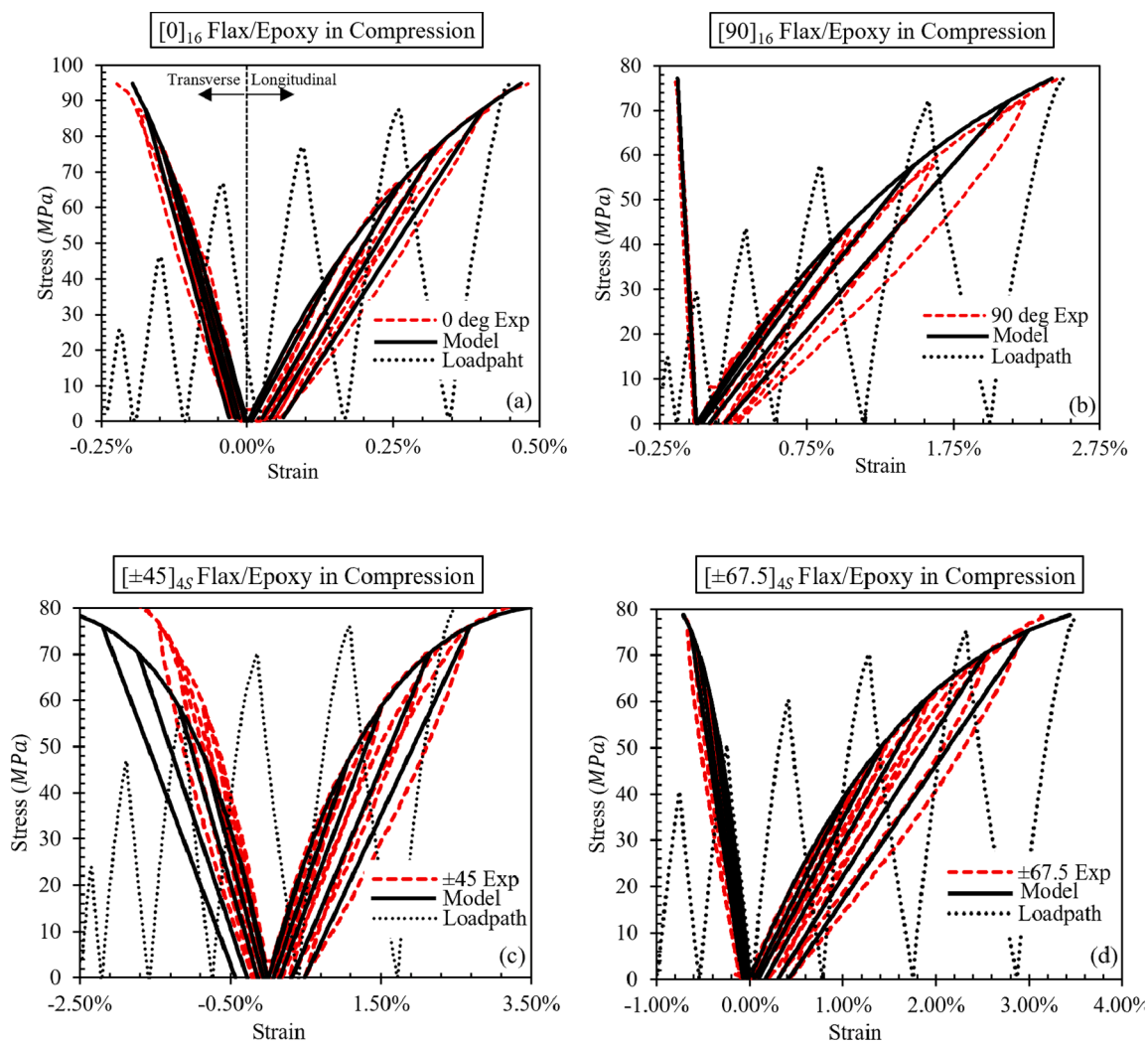

Fig. 9. Comparison of Flax/Epoxy experimental material response (red) and model simulation (black) for: (a) $[0]_{16}$, (b) $[90]_{16}$, (c) $[\pm45]_{4s}$, and (d) $[\pm67.5]_{4s}$ laminates. (For interpretation of the references to colour in this figure legend, the reader is referred to the web version of this article.)

4.4. Future prospects

A distinct feature associated with this model is that the damage and plasticity effects of ply interface are not individually quantified. Rather, the damage and plasticity state of each ply and its corresponding interface is considered as one. Unaccounted damage mechanisms such as inter-ply delamination or ply rotation for example, could be studied by the addition of interface-specific constitutive equations as shown in [70,71]. Kink band formation and inter-fibril crack propagation could be studied by further discretizing the damage constitutive equations into separate micromechanical equations with individual damage variables and evolution laws much like in the works of Sliseris et al. [59].

In this study, all experimental tests were performed at room temperature with an applied strain rate of 2 mm/min. Poilane et al. [58] have shown through creep tests that NFC behavior is sensitive to the applied strain rate and ambient temperature. Significant strength and stiffness loss were observed with an increase in applied strain rate at temperatures above 50 °C. As these relationships were identified to be proportional, and the failure strain was found to be relatively constant, it is possible that strain rate and temperature effects could be accounted for with a modulus (E) correction factor.

A major long-term goal for this model is to expand its versatility. It has shown potent at simulating flax/epoxy behavior; therefore, it should be capable of simulating other nonlinearly behaving NFCs. This will require the performance of mechanical testing to quantify the material behavior and to derive the associated material-specific parameters. Once obtained, this model would be capable of simulating a large variety of composites with minimal to no modifications. Lastly, the model as is, simulates a single volumetric (3D) element. Therefore, another future goal associated with this model is to integrate it into a finite element design software such as ABAQUS, and to expand its applications to multi-element structures.

5. Conclusion

Natural fibers present an untapped source of environmentally friendly, sustainable, and cost-effective substitutes to synthetic fibers used for composite reinforcement. Flax fibers have been shown to have comparable mechanical properties to E-Glass, the most popular choice of fiber reinforcement. The impeding factors against the widespread use of NFC as load-bearing components are the paucity of data on their mechanical behavior in compression and the absence of robust and accurate predictive tools.

In this research work, quasi-static compressive testing was performed on Flax/Epoxy laminates of four principle layups: $[0]_{16}$, $[90]_{16}$, $[\pm 45]_{4S}$ and $[\pm 67.5]_{4S}$. The experimental data was used to characterize their material behaviour in compression, with emphasis on stiffness and plasticity evolution. It was observed that flax/epoxy laminates exhibit linear damage evolution and power-law plasticity evolution behaviors. This information was used to develop a thermodynamic CDM-based model captured the overall nonlinear behavior of NFCs. The standard mesoscale damage theory was modified according to the experimental observations to include damage and plasticity evolution in all three orthotropic directions. The modified theory was incorporated into open-source SMART+ material libraries, and the global laminate response was integrated using a multi-scale periodic homogenization scheme.

The resulting model presented was validated on flax/epoxy composites in compression, as well as on E-glass composites in tension and compression. The model was shown to be a robust and versatile predictive tool via the simulation of the mechanical response of composites with various fiber orientation. Overall, the Modified Mesoscale Damage Model was found to be suitable for predicting the compressive behavior of both synthetic and natural fiber composites. The ability to accurately model the nonlinear mechanical behavior of NFCs will increase the confidence of engineers and designers in the capabilities of NFC parts and components. Thus, further promote the use of sustainable and environmentally friendly materials for structural applications.

Author contributions

Zia Mahboob and Constantin Nicolinco were involved, specimen preparation, experimental testing, data analysis, and/or first draft preparation. Yves Chemisky and Fodil Meraghni were involved in coding and algorithm implementation. Donatus Oguamanam were involved in manuscript writing/editing. Habiba Bougherara, was involved in study design, critical data analysis, manuscript editing. Habiba Bougherara is the main supervisor, project administrator, and the responsible for funding acquisition and resources.

Declaration of Competing Interest

The authors declare that they have no known competing financial interests or personal relationships that could have appeared to influence the work reported in this paper.

Acknowledgements

The authors extend their gratitude to Huntsman Corporation (The Woodlands, TX, USA) for supplying the epoxy resin and hardener. The authors also thank Messrs. David Miller and Andrei Betlen for their expertise and support with software debugging and implementation.

References

[1] Garkhail S, Heijenrath R, Peijs T. Mechanical properties of natural-fibre-mat-reinforced thermoplastics based on flax fibres and polypropylene. Appl Compos Mater 2000;7:351–72.

[2] Joshi SV, Drzal L, Mohanty A, Arora S. Are natural fiber composites environmentally superior to glass fiber reinforced composites? Compos A Appl Sci Manuf 2004;35:371–6.

[3] Faruk O, Bledzki AK, Fink HP, Sain M. Biocomposites reinforced with natural fibers: 2000–2010. Prog Polym Sci 2012;37:1552–96.

[4] Dittenber DB, GangaRao HV. Critical review of recent publications on use of natural composites in infrastructure. Compos A Appl Sci Manuf 2012;43:1419–29.

[5] Le Duigou A, Davies P, Baley C. Environmental impact analysis of the production of flax fibres to be used as composite material reinforcement. J Biobased Mater Bioenergy 2011;5:153–65.

[6] Corbière-Nicollier T, Laban BG, Lundquist L, Leterrier Y, Månson JA, Jolliet O. Life cycle assessment of biofibres replacing glass fibres as reinforcement in plastics. Resour Conserv Recycl 2001;33:267–87.

[7] Pickering KL, Efendy MA, Le TM. A review of recent developments in natural fibre composites and their mechanical performance. Compos A Appl Sci Manuf 2016;83:98–112.

[8] Wambua P, Ivens J, Verpoest I. Natural fibres: can they replace glass in fibre reinforced plastics? Compos Sci Technol 2003;63:1259–64.

[9] Satyanarayana KG, Arizaga GG, Wypych F. Biodegradable composites based on lignocellulosic fibers—an overview. Prog Polym Sci 2009;34:982–1021.

[10] Liang S, Gning PB, Guillaumat L. A comparative study of fatigue behaviour of flax/epoxy and glass/epoxy composites. Compos Sci Technol 2012;72:535–43.

[11] Shah DU. Developing plant fibre composites for structural applications by optimising composite parameters: a critical review. J Mater Sci 2013;48:6083–107.

[12] Bodros E, Pillin I, Montrelay N, Baley C. Could biopolymers reinforced by randomly scattered flax fibre be used in structural applications? Compos Sci Technol 2007;67:462–70.

[13] Ng HM, Sin LT, Tee TT, Bee ST, Hui D, Low CY, et al. Extraction of cellulose nanocrystals from plant sources for application as reinforcing agent in polymers. Compos B Eng 2015;75:176–200.

[14] Węcławski BT, Fan M, Hui D. Compressive behaviour of natural fibre composite. Compos B Eng 2014;67:183–91.

[15] Cheung HY, MP, Ho KT, Lau Cardona F, Hui D. Natural fibre-reinforced composites for bioengineering and environmental engineering applications. Compos Part B: Eng 2009;40: 655-663.

[16] Pil L, Bensadoun F, Pariset J, Verpoest I. Why are designers fascinated by flax and hemp fibre composites? Compos A Appl Sci Manuf 2016;83:193–205.

[17] Shah DU. Natural fibre composites: comprehensive Ashby-type materials selection charts. Mater Des (1980–2015) 2014;62:21–31.

[18] Zsiros JA. Natural fibers and fiberglass: a technical and economic comparison. Ph. D. thesis, Brigham Yound University; 2010.

[19] Stamboulis A, Baillie C, Peijs T. Effects of environmental conditions on mechanical and physical properties of flax fibers. Compos A Appl Sci Manuf 2001;32:1105–15.

[20] El-Sabbagh A, Steuernagel L, Ziegmann G, Meiners D, Toepfer O. Processing parameters and characterisation of flax fibre reinforced engineering plastic composites with flame retardant fillers. Compos B Eng 2014;62:12–8.

[21] Newman RH. Auto-accelerative water damage in an epoxy composite reinforced with plain-weave flax fabric. Compos A Appl Sci Manuf 2009;40:1615–20.
[22] Alix S, Philippe E, Bessadok A, Lebrun L, Morvan C, Marais S. Effect of chemical treatments on water sorption and mechanical properties of flax fibres. Bioresour Technol 2009;100:4742–9.
[23] Assarar M, Scida D, El Mahi A, Poilâne C, Ayad R. Influence of water ageing on mechanical properties and damage events of two reinforced composite materials: flax–fibres and glass–fibres. Mater Des 2011;32:788–95.
[24] Hagstrand PO, Oksman K. Mechanical properties and morphology of flax fiber reinforced melamine-formaldehyde composites. Polym Compos 2001;22:568–78.
[25] Lu T, Jiang M, Jiang Z, Hui D, Wang Z, Zhou Z. Effect of surface modification of bamboo cellulose fibers on mechanical properties of cellulose/epoxy composites. Compos Part B Eng 2013;51:28–34.
[26] Spārniņš E, Nyström B, Andersons J. Interfacial shear strength of flax fibers in thermoset resins evaluated via tensile tests of UD composites. Int J Adhes Adhes 2012;36:39–43.
[27] Thuault A, Domengès B, Hervas I, Gomina M. Investigation of the internal structure of flax fibre cell walls by transmission electron microscopy. Cellulose 2015;22: 3521–30.
[28] Liu Q, Stuart T, Hughes M, Sharma H, Lyons G. Structural biocomposites from flax–Part II: the use of PEG and PVA as interfacial compatibilising agents. Compos A Appl Sci Manuf 2007;38:1403–13.
[29] Baley C. Analysis of the flax fibres tensile behaviour and analysis of the tensile stiffness increase. Compos A Appl Sci Manuf 2002;33:939–48.
[30] Xie X, Zhou Z, Jiang M, Xu X, Wang Z, Hui D. Cellulosic fibers from rice straw and bamboo used as reinforcement of cement-based composites for remarkably improving mechanical properties. Compos B Eng 2015;78:153–61.
[31] Hughes M, Carpenter J, Hill C. Deformation and fracture behaviour of flax fibre reinforced thermosetting polymer matrix composites. J Mater Sci 2007;42: 2499–511.
[32] Coroller G, Lefeuvre A, Le Duigou A, Bourmaud A, Ausias G, Gaudry T, et al. Effect of flax fibres individualisation on tensile failure of flax/epoxy unidirectional composite. Compos A Appl Sci Manuf 2013;51:62–70.
[33] Bos H, Donald A. In situ ESEM study of the deformation of elementary flax fibres. J Mater Sci 1999;34:3029–34.
[34] Lamy B, Pomel C. Influence of fiber defects on the stiffness properties of flax fibers-epoxy composite materials. J Mater Sci Lett 2002;21:1211–3.
[35] Liang S, Gning PB, Guillaumat L. Properties evolution of flax/epoxy composites under fatigue loading. Int J Fatigue 2014;63:36–45.
[36] Mahboob Z, El Sawi I, Zdero R, Fawaz Z, Bougherara H. Tensile and compressive damaged response in Flax fibre reinforced epoxy composites. Compos A Appl Sci Manuf 2017;92:118–33.
[37] Charlet K, Eve S, Jernot J, Gomina M, Breard J. Tensile deformation of a flax fiber. Procedia Eng 2009;1:233–6.
[38] Romhany G, Karger-Kocsis J, Czigany T. Tensile fracture and failure behavior of technical flax fibers. J Appl Polym Sci 2003;90:3638–45.
[39] Shah DU. Damage in biocomposites: stiffness evolution of aligned plant fibre composites during monotonic and cyclic fatigue loading. Compos A Appl Sci Manuf 2016;83:160–8.
[40] Choudhury AR. Environmental impacts of the textile industry and its assessment through life cycle assessment. In: Roadmap to Sustainable Textiles and Clothing. Springer; 2014. p. 1-39.
[41] Dittenber DB, GangaRao HVS. Critical review of recent publications on use of natural composites in infrastructure. Compos A Appl Sci Manuf 2012;43(8): 1419–29.
[42] Graupner N, Herrmann AS, Mussig J. Natural and man-made cellulose fibre-reinforced poly(lactic acid) (PLA) composites: an overview about mechanical characteristics and application areas. Compos A Appl Sci Manuf 2009;40:810–21.
[43] Bos HL, Müssig J, van den Oever MJ. Mechanical properties of short-flax-fibre reinforced compounds. Compos A Appl Sci Manuf 2006;7:1591–604.
[44] Mahboob Z, Chemisky Y, Meraghni F, Bougherara H. Mesoscale modelling of tensile response and damage evolution in natural fibre reinforced laminates. Compos B Eng 2017;119:168–83.
[45] Bos H, Van Den Oever M, Peters O. Tensile and compressive properties of flax fibres for natural fibre reinforced composites. J Mater Sci 2002;37:1683–92.
[46] Hughes M. Defects in natural fibres: their origin, characteristics and implications for natural fibre-reinforced composites. J Mater Sci 2012;47:599–609.
[47] Aslan M, Chinga-Carrasco G, Sørensen BF, Madsen B. Strength variability of single flax fibres. J Mater Sci 2011;46:6344–54.
[48] Mukherjee P, Satyanarayana K. An empirical evaluation of structure-property relationships in natural fibres and their fracture behaviour. J Mater Sci 1986;21: 4162–8.
[49] Lamy B, Baley C. Stiffness prediction of flax fibers-epoxy composite materials. J Mater Sci Lett 2000;19:979–80.
[50] Wind turbine made of 100% natural materials. JEC Innovation Awards Programme; 2010.
[51] Stuttgart University tests natural fibre wind turbine blades. Renewable Energy Magazine; 2014. Available: https://www.renewableenergymagazine.com/wind/stuttgart-university-tests-natural-fibre-wind-turbine-20140312.
[52] Milne I, Ritchie R, Karihaloo B, editors. Comprehensive Structural Integrity, vol. 10, New York: Elsevier; 2003.
[53] Herakovich CT. Mechanics of fibrous composites. New York: John Wiley & Sons; 1998. p. 332–61.
[54] Allix O, Ladeveze P, Corigliano A. Damage analysis of interlaminar fracture specimens. Compos Struct 1995;31:61–74.
[55] Facca AG, Kortschot MT, Yan N. Predicting the elastic modulus of natural fibre reinforced thermoplastics. Compos A Appl Sci Manuf 2006;37:1660–71.
[56] Andersons J, Modniks J, Spārniņš E. Modeling the nonlinear deformation of flax-fiber-reinforced polymer matrix laminates in active loading. J Reinf Plast Compos 2015;34:248–56.
[57] Panamoottil SM, Das R, Jayaraman K. Anisotropic continuum damage model for prediction of failure in flax/polypropylene fabric composites. Polym Compos 2016; 37:2588–97.
[58] Poilâne C, Cherif Z, Richard F, Vivet A, Doudou BB, Chen J. Polymer reinforced by flax fibres as a viscoelastoplastic material. Compos Struct 2014;112:100–12.
[59] Sliseris J, Yan L, Kasal B. Numerical modelling of flax short fibre reinforced and flax fibre fabric reinforced polymer composites. Compos B Eng 2016;89:143–54.
[60] Standard, A. S. T. M. D6641/D6641M-14. Standard Test Method for Compressive Properties of Polymer Matrix Composite Materials Using a Combined Loading Compression (CLC) Test Fixture. ASTM International, West Conshohocken, PA; 2014.
[61] Standard, A. S. T. M. 695 Standard Test Method for Compressive Properties of Rigid Plastics. ASTM materials standards; 2002.
[62] Ladeveze P, LeDantec E. Damage modelling of the elementary ply for laminated composites. Compos Sci Technol 1992;43:257–67.
[63] Lemaitre J, Chaboche JL. Damage mechanics. In: Mechanics of Solid Materials. Cambridge: Cambridge University Press; 1990. p. 346–450.
[64] SMART+ Smart Materials Algorithms and Research Tools. Available: http://www.lem3.univ-lorraine.fr/chemisky/smartplus/.
[65] Simo J, Hughes T. Computational inelasticity, Interdisciplinary Applied Mathematics, vol. 7. New York: Springer-Verlag; 1998.
[66] Chatzigeorgiou G, Charalambakis N, Chemisky Y, Meraghni F. Periodic homogenization for fully coupled thermomechanical modeling of dissipative generalized standard materials. Int J Plast 2016;81:18–39.
[67] Storn R, Price K. Differential evolution–a simple and efficient heuristic for global optimization over continuous spaces. J Global Optim 1997;11:341–59.
[68] Optimization code from open source Spicy.org. Available: https://docs.scipy.org/doc/scipy/reference/generated/scipy.optimize.differential_evolution.html#r108fc14fa019-1.
[69] Amijima S, Adachi T. Nonlinear stress-strain response of laminated composites. J Compos Mater 1979;13:206–18.
[70] Allix O, Ladevèze P. Interlaminar interface modelling for the prediction of delamination. Compos Struct 1992;22:235–42.
[71] Daghia F, Ladeveze P. Identification and validation of an enhanced mesomodel for laminated composites within the WWFE-III. J Compos Mater 2013;47:2675–93.